

The orientation and bonding of CO on Mo(100) using angle-resolved photoelectron spectroscopy and near-edge x-ray absorption fine structure

J. P. Fulmer, F. Zaera,^{a)} and W. T. Tysoe

Department of Chemistry and Laboratory for Surface Studies, University of Wisconsin-Milwaukee, Milwaukee, Wisconsin 53201

(Received 24 June 1987; accepted 4 September 1987)

The nature of the species formed by CO chemisorption of Mo(100) has been investigated using angle-resolved ultraviolet photoelectron spectroscopy (ARUPS) and near-edge x-ray absorption spectroscopy. High-resolution electron energy loss spectroscopy (HREELS) indicates the formation of two distinct types of CO. At coverages greater than 50% of saturation, chemisorbed CO exhibits a CO stretching frequency of $\sim 2100\text{ cm}^{-1}$ corresponding to a CO molecule chemisorbed in an atop site. ARUPS indicates that at these coverages CO chemisorbs with its axis perpendicular to the surface in an analogous manner to that commonly observed on transition metal surfaces. At coverages less than 50% of saturation, CO exhibits an extraordinarily low stretching frequency of $\sim 1200\text{ cm}^{-1}$. Both NEXAFS and ARUPS measurements unequivocally indicate that at low coverages CO is tilted at $\sim 40^\circ$ to the surface normal. Since CO is tilted with respect to the surface at low coverages, this effect cannot be ascribed to adatom-adatom interactions, and a careful measurement of the positions of the photoelectron peaks of the tilted molecule indicates that both the 1π and the 5σ orbitals participate in surface bonding. A bonding model is proposed that is in accord with these observations in which the CO molecule chemisorbs into a fourfold hollow site.

I. INTRODUCTION

Carbon monoxide chemisorbs onto transition metal surfaces, in the majority of cases, with the carbon-oxygen bond perpendicular to the sample surface, exhibiting a C-O stretching frequency at around 2000 cm^{-1} ; the exact value of this stretching frequency depending on whether the CO chemisorbs at an atop, bridging, or hollow site. The bonding of CO, its dissociation probability, and the effect of alkalis on CO chemisorption have all been explained in terms of the Blyholder model⁸ in which the molecule surface bond is formed by electron donation to the surface from the CO 5σ orbital, with a synergistic backbond from the surface into the CO $2\pi^*$ antibonding orbital. Variations in CO chemistry can be rationalized from changes in work function (either by changing the metal or adding an alkali) which in turn alters the relative proportions of 5σ donation compared to $2\pi^*$ back donation. Cases in which the chemisorbed CO tilts with respect to the surface normal can be ascribed to adatom-adatom interactions which produce glide planes in the ordered overlayer. Such adatom-adatom interactions occur at high coverages.¹ Recently, however, vibrational spectroscopy in the form of high-resolution electron energy loss spectroscopy (HREELS) has revealed a new frequency ($\sim 1200\text{ cm}^{-1}$) CO mode at low coverage. This has been tentatively assigned to the vibration of a tilted CO molecule, but since this species is observed at low CO coverages cannot be ascribed to a molecule that is tilted because of adatom-adatom interactions. Such low vibrational frequencies at low coverage have hitherto been observed for CO adsorbed on Fe(100),² Cr(110),³ and Mo(100).⁶ NEXAFS spectra for CO on Fe(100) indicated that the so-called α_3 state of CO

comprises a molecule that is tilted at 45° to the surface normal.⁴ Tilted molecular species have been proposed for CO chemisorbed onto Cr(110) based on electron stimulated desorption (ESDIAD) experiments³ and ultraviolet photoelectron spectroscopy data.⁷ Recent theoretical calculations have concluded that the stable molecular orientation on Cr(110) is when the molecular axis of CO is parallel to the surface and in which the 4σ , 1π , and 5σ orbitals of CO all interact with the surface.⁵

Another example of a surface that exhibits this low frequency mode following CO chemisorption is Mo(100).⁶ This low frequency state, which formally corresponds to a CO bond order of unity, has been further shown by combining thermal desorption spectroscopy (TDS) and HREELS studies to be a precursor to CO dissociation. The data of Ref. 6 show that at a CO coverage of 0.4 (where coverage in this case signifies relative coverage, i.e., $\theta/\theta_{\text{max}}$) the HREELS spectrum exhibits almost exclusively the low frequency CO stretching modes, and in TDS two high temperature desorption peaks due to second-order atom recombination reaction are observed. A very small peak at $\sim 2000\text{ cm}^{-1}$ at this coverage ($\theta/\theta_{\text{max}} = 0.4$) suggests that a small portion of the CO chemisorbs at an atop site. Increasing the exposure so that the CO coverage is 0.65 produces a spectrum in which both the low frequency (1200 cm^{-1}) and high frequency (2000 cm^{-1}) loss peaks increase in intensity, suggesting a simultaneous population of both of these states in this coverage range (i.e., between $\theta/\theta_{\text{max}} = 0.4$ and $\theta/\theta_{\text{max}} = 0.65$). Further exposure results only in an increase of the 2000 cm^{-1} peak. This suggests that the "low frequency" CO covers approximately half the surface, the other half being CO chemisorbed at an atop site. Auger measurements suggest a saturation CO coverage of $\sim 1.8 \times 10^{15}$ molecules/cm²; this corresponds to approximately 2 CO molecules per surface molybdenum atom on the (100) face.

^{a)} Department of Chemistry, University of California, Riverside, CA 92521.

We present in the following angle-resolved ultraviolet photoelectron spectroscopic (ARUPS) and near-edge x-ray absorption fine structure (NEXAFS) measurements for CO on Mo(100). The NEXAFS data suggest that the molecule is tilted at $40^\circ \pm 10^\circ$ to the surface normal. Angle-resolved photoelectron spectroscopy also indicates that the molecule is tilted at $40^\circ \pm 5^\circ$ to the plane of the Mo(100) surface. Measurement of the spacing between the $2\pi^*$ and $6\sigma^*$ resonances in NEXAFS suggests that the CO bond is some $0.25 \pm 0.05 \text{ \AA}$ longer in the tilted orientation than for the "perpendicular" molecule. This longer CO bond is in accord with the weaker CO force constant observed in HREELS.

The positions of the CO energy levels in UPS for the perpendicular and tilted CO molecules are quite different, and the data suggest that while there is a strong component of bonding which involves donation of 5σ electrons to the surface for tilted CO, 1π electron density is also donated to the surface. Comparison with organometallic analogs suggests that σ and π donation are to adjacent surface molybdenum atoms. This molecular geometry is somewhat different to that predicted theoretically for the chemisorption of CO on Cr(110).⁵

II. EXPERIMENTAL

These experiments were performed at the National Synchrotron Light Source at Brookhaven National Laboratory on beamline U14A. The monochromator used for these experiments was a PGM which has been described in detail elsewhere.⁹

The ion pumped stainless steel vacuum chamber used in these experiments operated at a base pressure of 1×10^{-10} Torr after bakeout. It was equipped with a cylindrical mirror analyzer for Auger analysis of the surface which was mainly used to establish sample cleanliness and for near-edge x-ray absorption fine structure (NEXAFS) experiments. It also contained a rotatable angle-resolving hemispherical analyzer for photoelectron spectroscopy experiments.

The Mo(100) crystal was prepared using standard metallographic techniques and was mounted to the sample manipulator via tantalum wires spotwelded to the edge of the crystal. The sample could be resistively heated to 2000 K and cooled to $\sim 120 \text{ K}$ via thermal contact to a liquid nitrogen reservoir. The sample was cleaned using standard procedures, i.e., by repeatedly annealing in 1×10^{-7} Torr of oxygen at 1200 K to remove carbon, and heating to 2000 K *in vacuo* to remove oxygen. The CO used in these studies was vacuum distilled several times to remove contaminants (predominantly metal carbonyls) and stored in glass. The CO was free of impurities as adjudged by mass spectroscopy.

Preliminary photoemission experiments were performed to establish the photon energy that optimized the adsorbate signal relative to those from the substrate, as well as overall count rates. Photon energies of 40 eV were used for photoelectron spectroscopy throughout this work. This has been shown previously to be close to the optimum energy for UPS of CO on transition metal surfaces.¹⁰ Photoelectron spectra were obtained in a pulse counting mode with a fixed analyzer pass energy of 20 eV (corresponding to an analyzer resolution of 0.2 eV). The monochromator resolution at the

photon energies used (40 eV) was measured to be 0.2 eV.

NEXAFS spectra were taken in the majority of cases using Auger detection. A peak-to-peak modulation amplitude of 30 V was used in order to degrade the resolution of electrons photoejected from just below the Fermi edge.¹¹ Nevertheless, this renders the background in the region of the $1s$ to 6σ resonances less reliable, so that quantitative measurements of intensities of these features was avoided in the data analysis. A set of spectra were also taken using the crystal current as a measure of the adsorption.

III. RESULTS

Figure 1 shows a series of angle-resolved photoelectron spectra of a Mo(100) surface following exposure to 0.5 L ($1 \text{ L} = 10^{-6} \text{ Torr s}$) of CO at 120 K taken with the photoelectron detection angle normal to the surface while varying the angle of incidence of the UV beam. The definitions of the angles used in this paper are shown in Fig. 2. According to previous work,⁶ this CO exposure corresponds to a coverage, $\theta/\theta_{\text{sat}} \sim 0.5$, i.e., 50% of saturation coverage. Chemisorbed CO in this low coverage state exhibits low CO stretching frequencies and dissociates upon heating. The spectra are normalized to total incident photon flux which was determined by measuring sample current to ground. These spectra exhibit a broad feature between 7 and 14 eV below the Fermi edge due to chemisorbed CO. It is evident that the shape of this feature changes only little as a function of incidence angle. Shown for comparison are the spacings of the photoemission peaks from the 4σ , 1π , and 5σ orbitals of gas phase CO. These lines are rigidly shifted so that the 5σ level aligns with the CO photoemission peak at $\sim 13 \text{ eV}$ binding energy. The structure between the Fermi edge (denoted as

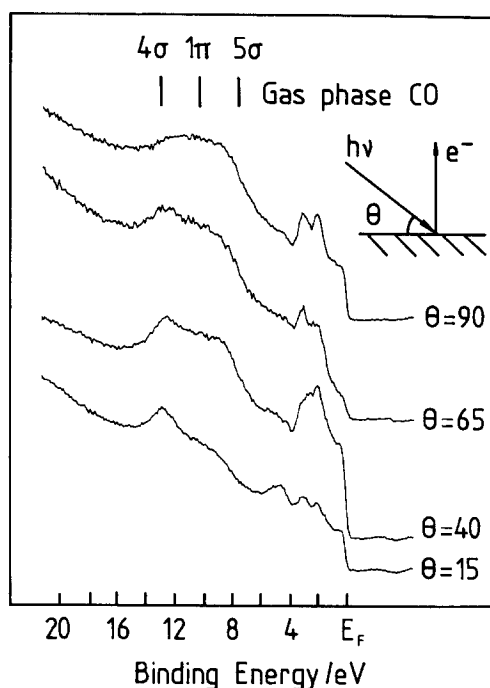
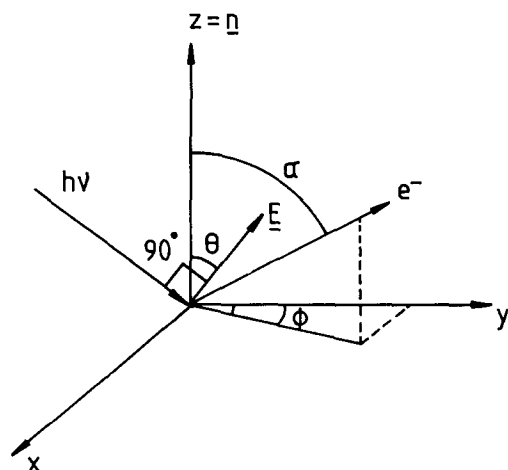


FIG. 1. Photoelectron spectra of 0.5 L of CO on Mo(100) taken at normal emission as a function of photon incidence angle. The photon energy was 40 eV.



Surface is in the x - y plane
 \hat{n} Surface normal

FIG. 2. Coordinate system used for the analysis of the UPS and NEXAFS data.

E_F in the diagram) and 4 eV binding energy is due to emission from the substrate d electrons.

A similar set of spectra (i.e., normal detection, taken as a function of photon incidence angle) are shown in Fig. 3 for a surface saturated with CO (5 L exposure) at 120 K. CO photoemission features in this case are significantly more intense than the spectra of Fig. 1 reflecting a higher total CO coverage. The spectrum consists of two features that are reasonably well resolved; a narrow peak 11.9 eV below the Fermi level and a broader peak at ~ 8.7 eV below the Fermi level. These peak positions are in reasonable agreement with

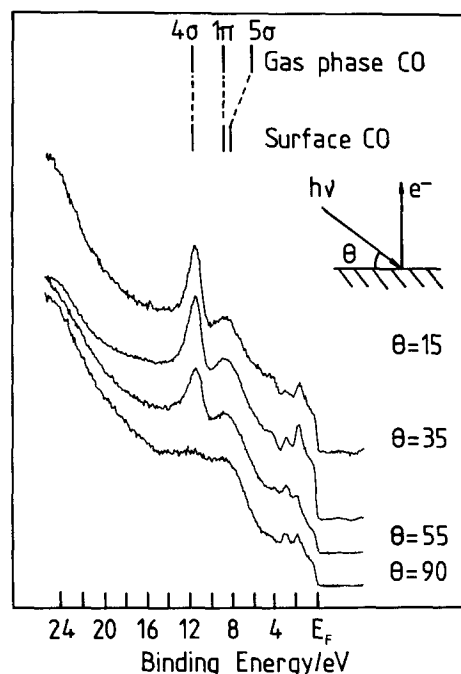


FIG. 3. Photoelectron spectra of a saturation coverage of CO on Mo(100) (5 L) taken at normal emission as a function of photon incidence angle. The photon energy was 40 eV.

spectra observed for CO on group VIII transition metal surfaces [e.g., CO/Ni(100)¹²]. The peak at 11.9 eV below E_F shows a significant variation in intensity as a function of incidence angle, while the broad peak at 8.7 eV below the Fermi edge shows little variation in intensity. Again shown for comparison are the positions of the peaks in the gas phase CO photoelectron spectrum, and the positions of the peaks for chemisorbed CO. The assignment of these peaks will be discussed below.

Figure 4 shows a series of spectra following a 5 L exposure of CO (i.e., a saturated surface) as a function of photoelectron emission angle taken with the light beam normal to the surface. Spectra are shown as a function of azimuthal angle both in the plane and perpendicular to the plane of polarization, and again the positions of gas phase and chemisorbed photoemission peaks are shown for comparison. While the broad peak shows little variation in shape as a function of azimuthal angle perpendicular to the plane of polarization significant variation in the shapes of the photoemission profiles with azimuthal angle parallel to the plane is evident. Figure 5 shows a set of spectra taken as a function of parallel azimuthal detection angle for normal incidence following 0.5 L CO exposure. In this case there is some variation in total intensity and a slight variation in the shape of the photoemission envelope from chemisorbed CO.

Near edge x-ray absorption fine structure (NEXAFS) spectra of a surface saturated with CO (5 L exposure at 120 K) were taken for both normal and grazing incidence (70° to the surface normal). Figure 6 shows the π resonances at the C 1s and O 1s absorption edges (i.e., C 1s to $2\pi^*$ and O 1s to $2\pi^*$ transitions, respectively) for normal and grazing incidence. The absorption cross sections in this case were measured from the intensity of the O(*KLL*) and C(*KLL*) Auger decay pathways of the respective core holes. These data indi-

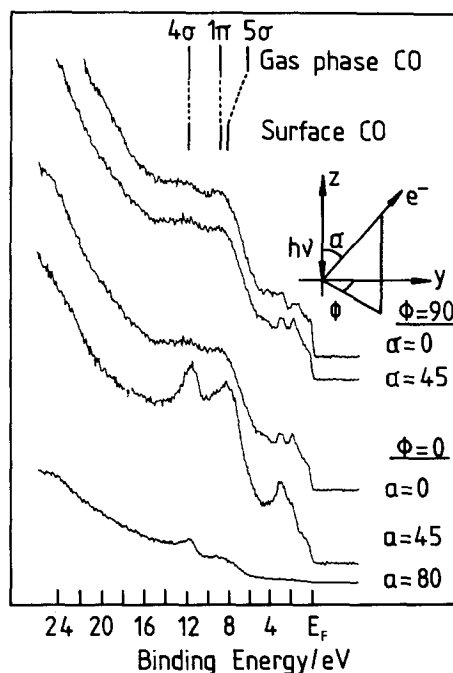


FIG. 4. Normal incidence photoelectron spectra following exposure to 5 L CO (i.e., a saturated surface) as a function of azimuthal detection angles.

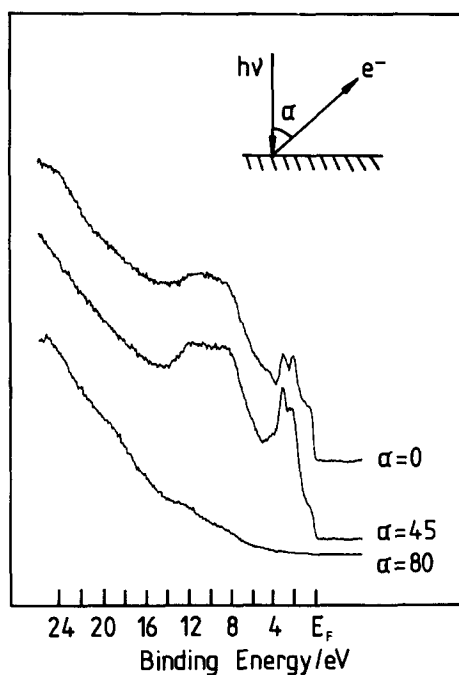


FIG. 5. Normal incidence photoelectron spectra following exposure to 0.5 L CO (50% of saturation) as a function of azimuthal (α , $\phi = 0$) detection angles in the plane of polarization only.

cate that there is still a significant absorption into the $2\pi^*$ level at grazing incidence (70° to the surface normal). Figure 7 shows the C edge NEXAFS spectrum in which the absorption was obtained by measuring the total current through the crystal. The data in this case are significantly noisier because of the inherently less sensitive detection method. However, the data in the region of the σ resonance is more reliable than that obtained using the Auger detection technique since there is no likelihood of interference from photoemission from the d band.¹⁰ The spectrum at normal incidence exhibits a very broad σ resonance. The π - σ spacing in this case is 11 ± 1 eV. The grazing incidence σ - π spacing is significantly different from this value, and in this case is 19 ± 1 eV.

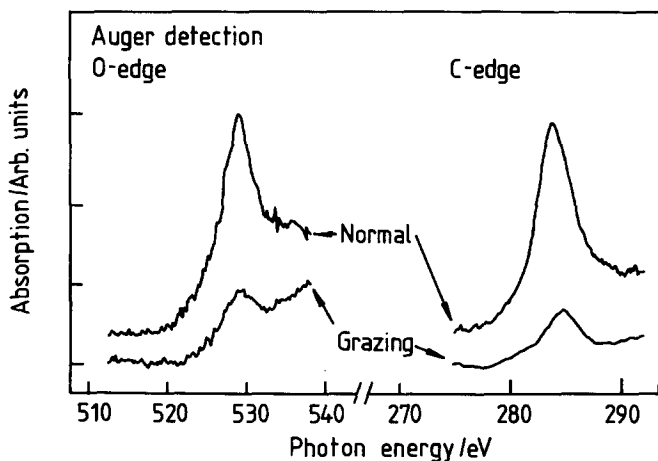


FIG. 6. Near-edge x-ray absorption fine-structure experiment showing π resonances at the O edges and C edge for a Mo(100) surface saturated with CO.

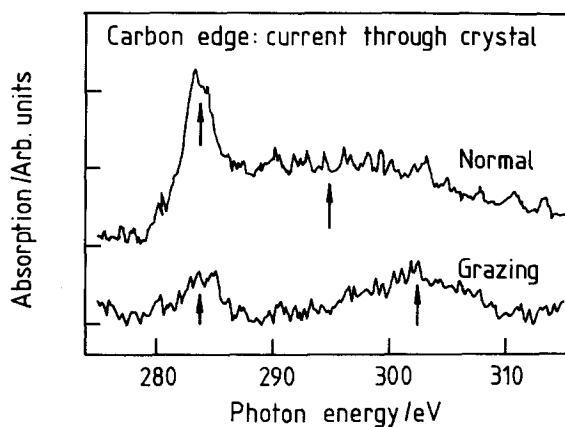


FIG. 7. NEXAFS spectra of a CO saturated Mo(100) surface obtained by measuring the current to ground through the crystal.

IV. DISCUSSION

We turn our attention initially to determining the angle of the low coverage CO state with respect to the surface. The consensus in the literature is that such a low CO stretching frequency of this state suggests that this corresponds to a CO molecule chemisorbed with a C-O axis that is not perpendicular to the surface. Figure 6 shows the π resonances at both the carbon and oxygen edges. If the surface consisted entirely of CO bonded with its molecular axis normal to the surface, the ratio of absorption cross section at normal vs grazing incidence should be ~ 8.5 .¹³ Experimentally we obtain for this system a ratio between 3 and 4 indicating the coexistence of perpendicular and tilted CO molecules on the surface. The angular dependence of the NEXAFS for a $1s$ to $2\pi^*$ transition is proportional to¹³

$$\{4 - (3 \cos^2 \theta - 1)(3 \cos^2 t - 1)\},$$

where θ is the angle of incidence of the x rays (see Fig. 2), and t is the molecular tilt angle measured with respect to the surface normal. The NEXAFS data (Figs. 6 and 7) were taken for a molybdenum surface saturated with CO, so that approximately $50\% \pm 10\%$ of the surface consists of the species exhibiting a low CO stretching frequency (putatively tilted to the surface) and $50\% \pm 10\%$ consists of CO with the molecular axis perpendicular to the surface. Thus the ratio of perpendicular to tilted CO is between 40:60 and 60:40. The ratios of the normal to grazing absorption intensity for a $1s$ to $2\pi^*$ transition for a surface assumed to consist of either 60% perpendicular CO and 40% tilted CO (\bullet) and for a surface consisting of 40% perpendicular CO and 60% perpendicular CO (\times) (the extreme cases) are shown plotted in Fig. 8 as a function of CO tilt angle, t . Table I shows the measured values of the ratios of the absorbances for normal and grazing incidences taken from the data of Figs. 6 and 7 (i.e., for excitation from either the carbon or oxygen core levels). These ratios are shown plotted onto the theoretical curves of Fig. 8. The NEXAFS data therefore indicate that the CO is tilted at $40^\circ \pm 10^\circ$ to the surface normal.

The σ resonance at adsorption at the carbon edge was obtained by measuring the current through the crystal (Fig. 7). The σ resonance at glancing incidence is a broad feature

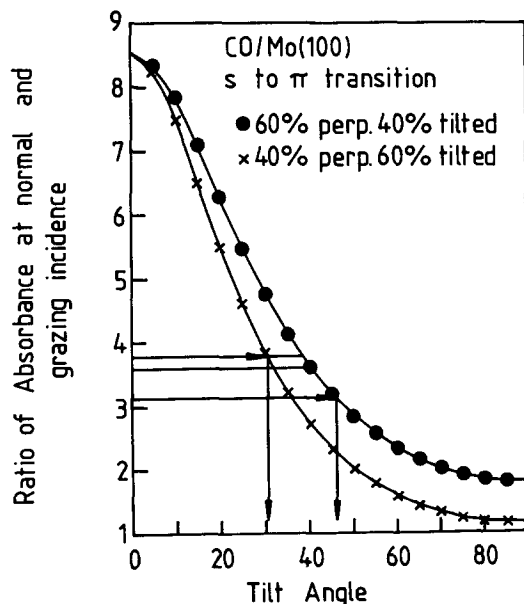


FIG. 8. Plot of the ratios of intensities of $1s$ to π^* transitions for normal grazing incidence as a function of molecular tilt angle for a surface consisting of 40% tilted CO and 40% perpendicular CO and 60% tilted and 40% perpendicular CO. Shown also are the experimental ratios taken from Table I and the tilt angles to which they correspond.

centered at 302 ± 1 eV photon energy and is primarily due to adsorption from the $1s$ to 6σ antibonding orbital of perpendicular CO. At normal incidence the corresponding feature is due to excitation into the 6σ level of *tilted* CO. The spacing between the σ and π resonances can be used as a measure of the CO bond length; empirically a shift of 1 eV in this spacing correlates with a change in a bond length of ~ 0.03 Å where a longer bond yields a smaller spacing between the σ and π resonances.¹⁴ Examination of the region in which the σ resonance occurs in the normal incidence experiment shows a broad plateau which starts to decrease above 300 eV photon energy. A possible interpretation of this feature is that it is an extremely broad σ resonance centered at 294 ± 1 eV photon energy. If this is indeed the case the change in σ to π spacing between a tilted and perpendicular CO molecule is 8 ± 2 eV, which implies that the tilted CO molecule has a CO bond some 0.25 ± 0.05 Å longer than the perpendicular CO. Such an increase in length of the CO bond for tilted CO would certainly be in line with the extremely low vibrational frequencies associated with this tilted state (~ 1200 cm^{-1}) and which corresponds, using bond order–bond frequency arguments, to a CO single bond.

The angular dependent UPS results complement the information obtained with NEXAFS. The photoelectron spectrum of a surface saturated with CO (which consists of $\sim 50\%$ tilted CO, and $\sim 50\%$ perpendicular CO) exhibits a sharp peak at 11.9 eV and a broad peak at 8.7 eV below the Fermi edge. The bonding of CO with its axis perpendicular to the metal surface is well understood. In general terms this is due to donation from the 5σ orbital, which is a nonbonding CO orbital consisting predominantly of a lone pair on carbon, into an empty metal d orbital, and a synergistic back donation from a filled metal d orbital into the $2\pi^*$ antibond-

TABLE I. NEXAFS π resonance intensity ratio as a function of incident angle for a CO saturated Mo(100) surface.

Spectrum	Normal to grazing intensity
6 (C edge)	3.63
6 (O edge)	3.12
7	3.80

ing orbital of CO. Herman and Bagus¹⁵ have calculated the shift in ionization energies of the CO valence orbitals in NiCO as a function of the Ni–C distance using the Hartree–Fock Δ SCF method. This shows that while the 4σ and 1π orbitals are only slightly stabilized as the CO molecule approaches the Ni atom, the 5σ orbital is *significantly* stabilized so that at sufficiently small Ni–C distances it can, in fact, become more stable than the 1π orbital. The relative ionization energies of these orbitals can be established using angle-resolved photoelectron spectroscopy in the case in which CO is bonded perpendicularly to the surface since the surface complex in this case has relatively high symmetry. This procedure is illustrated, for example, by the case of CO bonding on Ni(100).¹² An experimental geometry in which the normally emitted photoelectrons are detected and where the electric field is parallel to the surface (normal incidence) should exclude emission from the 4σ and 5σ levels of CO; electrons should be photoejected from the 1π orbitals only. As the incidence angle is varied from normal, the π levels increase in intensity since in this case there is a significant component of the electric field along the molecular axis. This increase in the σ -emission cross section is accompanied by a decrease in π -emission cross section. Such a set of experiments is shown in the data of Fig. 3. At normal incidence ($\theta = 90^\circ$), the photoelectron spectrum exhibits a broad peak at 8.7 eV below E_F which, in this geometry, must be due to emission from the 1π orbital. The small feature at 11.9 eV below E_F is due to some residual emission from the 4σ orbital of the tilted CO. As the light incidence angle is moved from normal incidence the emission cross section from the σ levels increases. The peak at 11.9 eV below E_F is therefore assigned to emission from the 4σ level of chemisorbed CO. The peak at 8.7 eV shifts slightly to 8.4 eV but its intensity remains almost constant. This is because the 1π and 5σ levels for chemisorbed CO are almost degenerate, so that the combined photoemission intensity remains almost constant. This is because the 1π and 5σ levels for chemisorbed CO are almost degenerate, so that the combined photoemission intensity from this accidentally degenerate $1\pi/5\sigma$ pair remains constant. The peak at 8.4 eV is therefore assigned to emission from the 5σ orbital of chemisorbed CO, and this suggests that in the case of CO on Mo(100) the 5σ level is not as strongly stabilized as for example in this case of CO on Ni(100). The positions of the peaks due to chemisorbed CO are shown in Figs. 3 and 4 and comparison with the positions of the peaks for gas phase CO indicates that the CO 5σ level is shifted due to bonding to the Mo surface by ~ 1 eV. The 4σ and 1π levels are not shifted in accord with the Blyholder model.

This phenomenon is further illustrated in the azimuthal plots of a CO saturated surface (Fig. 4). Calculations of the angular profiles of the σ orbitals of CO at normal incidence when it is perpendicularly bonded^{16,17} show that the photoemission cross section of a σ orbital should be zero at normal detection and increase with increasing polar angle, so that it reaches a maximum when the detection angle is 30° – 40° for an excitation energy of 40 eV, in accordance with our results. The spectra of Fig. 4 also serve to confirm the positions of the 4σ , 1π , and 5σ energy levels assigned above. No signal from the 4σ and 5σ peaks is expected when $\phi = 90$ regardless of α , in agreement with our results.

We return now to the low coverage state ($\theta/\theta_{\max} = 0.5$) of CO on Mo(100). NEXAFS data have shown that this corresponds to a CO molecule tilted at $40 \pm 10^\circ$ to the surface normal and with a CO bond some 0.25 \AA longer than perpendicular CO. Further corroboration of the low coverage CO orientation is furnished by the lack of variation in shape of the mainfold of photoemission peaks due to CO since this angle is reasonably close to the magic angle (54.7°). Figure 9 shows the normal detection photoemission spectra due to a tilted CO fitted to three Lorentzians. The experimental curves were obtained from the spectra of Fig. 1 by subtracting an estimated curved base line (due predominantly to inelastically scattered electrons). The background-subtracted data are shown plotted with identical heights; the vertical lines adjacent to each of the spectra represent the same count rates. The fitting parameters (width, position, and height) for the Lorentzians were allowed to vary independently. These values agree between

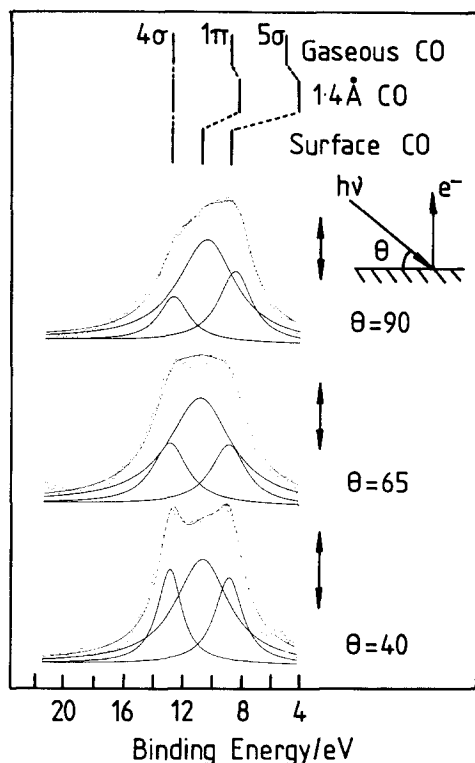


FIG. 9. Angle-resolved photoelectron spectra of 0.5 L of CO on Mo(100) replotted between 4 and 21 eV below E_F . An estimated background has been subtracted and the profiles fitted to three Lorentzians.

spectra taken at different incidence angles to within 10%. It is assumed that these peaks are due to emission from the 4σ , 1π , and 5σ CO orbitals. Because of the low symmetry of the tilted CO molecule, there are no longer any symmetry restrictions that require the 1π orbitals to be degenerate, so that formally these may split into two singly degenerate orbitals. However, calculations by Anderson⁵ for CO bonded *parallel* to the surface (in which case it would be expected that the splitting be a maximum) suggest that the fitted separation between these levels is $< 0.1 \text{ eV}$; below the resolution of the spectrometer. The binding energies of the peaks are 13.0 ± 0.1 , 10.9 ± 0.1 , and $9.0 \pm 0.1 \text{ eV}$ below the Fermi edge. The 13.0 eV binding energy peak is assigned to the 4σ orbital of CO as this is not involved in surface bonding to any large extent since it consists primarily of an oxygen lone pair, so that its binding energy would be expected to be close to that of perpendicular CO (11.9 eV). The 10.9 and 9.0 eV binding energy peaks are assigned to emission from the 1π and 5σ orbitals of chemisorbed CO, respectively.

The variation in intensity of photoemission peaks as a function of photon incidence angle can be used to confirm the NEXAFS measurements of molecular tilt angle. Shown plotted as solid lines in Fig. 10 is the theoretical variation of σ -photoemission intensity with incidence angle (normalized to 40° incidence) as a function of molecular tilt angle (measured with respect to the surface normal). Since the real and imaginary parts of the refractive index are likely to vary significantly from unity and zero, respectively, in UPS (i.e., for 40 eV photons), it was necessary to calculate the effect of the surface on the electric field. The theoretical plot in Fig. 10 was corrected for this effect by solving the Fresnel equations¹⁸ to yield the normal and perpendicular components of the electric field at a surface with a complex dielectric constant of $0.88 + i0.23$ as a function of photon incidence angle.

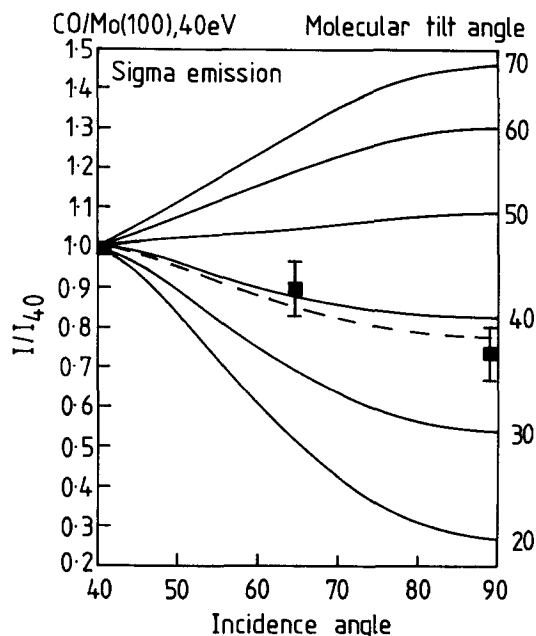


FIG. 10. Plot of photoemission intensity for emission from the CO 4σ level as a function of incidence angle. Plotted for comparison are theoretical curves of the same quantity for various values of tilt angle, taking into account the complex dielectric constant of the surface.

The component of the effective electric field along the molecular axis was calculated for different incidence and molecular tilt angles and averaged over all azimuthal angles. Shown also plotted on this curve are experimental points obtained from the fitted curves from Fig. 9 for the 13.0 eV peak (■). This yields a molecular tilt angle of $40^\circ \pm 5^\circ$; in good agreement with the value obtained from NEXAFS data. This also confirms that the 13.0 eV peak is due to emission from the 4σ orbital. Calculation of the molecular tilt angle *without* taking account of the complex refractive index of the molybdenum surface yields a molecular tilt angle of $\sim 50^\circ$, and illustrates the importance of this procedure. Analysis of the variation of intensity of the 1π and 5σ orbitals of the tilted CO was avoided, since the shift in the positions of these levels compared to gas phase CO suggests that they are strongly involved in binding to the molybdenum surface. This implies that the molecular orbitals associated with these peaks comprise a significant contribution from the substrate so that a variation of the intensity of these peaks as a function of incidence angle is likely to lead to erroneous estimated of tilt angle.

The plots of Fig. 5 show that the peak due to the 4σ orbital of tilted CO (at 13.0 eV binding energy) increases by a factor of ~ 1.5 as the detection angle changes from 0° to 45° . For a CO molecule tilted at 30° , and with 41 eV photons, the corresponding theoretical value of this ratio is ~ 2.1 .¹⁷ The emission intensity at 9.0 eV binding energy (assigned to emission from the 5σ orbital of tilted CO) increases by a factor of ~ 1.3 as the polar detection angle increases from 0° to 45° , again in accord with the theoretical calculations for tilted CO.

The data strongly suggest that both the 1π and the 5σ orbitals interact with the surface. Since both the 1π and 5σ peaks are shifted to higher binding energies for low coverage (tilted) CO compared to gas phase CO, this strongly suggests that both the 1π and the 5σ orbitals interact with the surface.

Organometallic compounds in which carbon monoxide is tilted at an angle with respect to the metal-metal bond¹⁹⁻²² have been synthesized. The bonding in these cases has been described by suggesting that the CO can behave as a four electron ligand by donating two electrons to each metal atom. Thus a pair of electrons is donated from the carbon lone pair (5σ orbital) and another electron pair from the 1π orbital. There appears therefore to be some correspondence between the bonding of CO to a Mo(100) surface and the bonding in these organometallic compounds. It should, however, be mentioned that the bridging CO stretching frequency in the organometallic compounds is ~ 1380 – 1400 cm^{-1} , substantially larger than the energy of the loss feature (~ 1200 cm^{-1}) observed for this species in HREELS and may reflect a considerably stronger bond for surface CO than in the complex.

We turn our attention finally to the question of nature of the CO adsorption site for tilted CO. The relatively large shifts in both 4σ and 1π orbitals on bonding require a geometry that allows simultaneous access of both of these orbitals to the surface. This suggests that tilted CO does *not* chemisorb at an atop site since this precludes significant simultaneous overlap of the 4σ and 1π orbitals with the surface. In

any case, CO chemisorbs in the atop site for coverages greater than 0.5, so that on this basis this geometry can be excluded as a possible binding for tilted CO. Of the remaining possibilities (bridge and hollow sites), adsorption at a hollow site seems most likely.

V. CONCLUSIONS

Two species have been identified on Mo(100) following CO adsorption at 120 K. At coverages up to $\sim 50\%$ of saturation, a species that has a characteristic vibrational frequency of ~ 1200 cm^{-1} and which on heating the sample leads to CO dissociation, has been unequivocally identified using NEXAFS and angle-resolved photoelectron spectroscopy as being tilted to the metal surface. The tilt angle has been measured at $40^\circ \pm 10^\circ$ to the surface normal using both NEXAFS and angle-resolved UPS. This species appears to bond via donation from the 5σ orbital to a molybdenum atom and also by donation of 1π electrons to an adjacent molybdenum atom. At higher coverages (approaching saturation) CO bonds with its axis perpendicular to the surface in a fashion that is identical to many transition metal surfaces. This CO has a characteristic vibrational frequency of ~ 2100 cm^{-1} , indicating adsorption at an atop site, and this species desorbs molecularly on heating. Finally, it is postulated that the tilted CO is adsorbed into a fourfold hollow site.

ACKNOWLEDGMENTS

We thank the donors of The Petroleum Research Fund, administered by the American Chemical Society, an Atlantic Richfield Foundation Grant of the Research Corporation and the University of Wisconsin-Milwaukee Graduate School for support of this research. We are also grateful to the personnel of NSLS, particularly Dr. M. Sagurton, for their assistance during these experiments.

¹R. M. Lambert, Surf. Sci. **49**, 325 (1975).

²D. W. Moon, S. L. Bernasek, and D. J. Dwyer, Surf. Sci. **163**, 215 (1985).

³N. D. Shinn and T. E. Madey, J. Chem. Phys. **83**, 5928 (1985).

⁴D. W. Moon, S. Cameron, F. Zaera, W. Eberhardt, R. Carr, S. L. Bernasek, J. L. Gland, and D. J. Dwyer, Surf. Sci. **180**, L123 (1987).

⁵S. P. Mehandru and A. B. Anderson, Surf. Sci. **169**, L281 (1986).

⁶F. Zaera, E. Kollin, and J. L. Gland, Chem. Phys. Lett. **121**, 464 (1985).

⁷N. D. Shinn and T. E. Madey, Phys. Rev. B **33**, 1464 (1986).

⁸G. Blyholder, J. Phys. Chem. **68**, 2772 (1964).

⁹G. P. Williams, M. R. Howells, N. Lucas, and P. A. Takas, Nucl. Instrum. Methods Phys. Res. A **222**, 99 (1984).

¹⁰E. W. Plummer and W. Eberhardt, Adv. Chem. Phys. **49**, 533 (1982).

¹¹J. Stohr, C. Noguera, and T. Kendelewicz, Phys. Rev. B **30**, 5571 (1984).

¹²R. J. Smith, J. Anderson, and G. J. Lapeyre, Phys. Rev. Lett. **37**, 1081 (1976).

¹³J. Stohr and R. Jaeger, Phys. Rev. B **26**, 4111 (1982).

¹⁴J. Stohr, J. L. Gland, W. Eberhardt, D. Outka, R. J. Madix, F. Sette, R. J. Koestner, and U. Doebler, Phys. Rev. Lett. **51**, 2414 (1983).

¹⁵K. Herman and P. Bagus, Phys. Rev. B **16**, 4195 (1977).

¹⁶J. W. Davenport, Phys. Rev. Lett. **36**, 945 (1976).

¹⁷D. Reiger, R. D. Schnell, and W. Steinmann, Surf. Sci. **143**, 157 (1984).

¹⁸J. A. Stratton, *Electromagnetic Theory* (McGraw-Hill, New York, 1941).

¹⁹C. P. Horowitz, E. M. Holt, C. P. Brock, and D. F. Shriver, J. Am. Chem. Soc. **107**, 8136 (1985).

²⁰F. A. Cotton, Prog. Inorg. Chem. **21**, 1 (1976).

²¹R. Colton and B. F. Hoskins, Aust. J. Chem. **28**, 1663 (1975).

²²C. J. Commons and B. F. Hoskins, Aust. J. Chem. **28**, 1673 (1975).